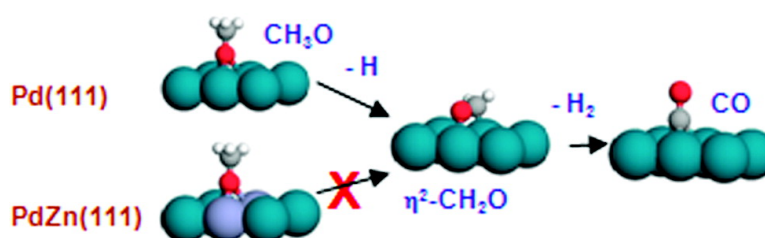


## Zn Modification of the Reactivity of Pd(111) Toward Methanol and Formaldehyde

Eseoghene Jeroro, and John M. Vohs

*J. Am. Chem. Soc.*, **2008**, 130 (31), 10199-10207 • DOI: 10.1021/ja8001265 • Publication Date (Web): 10 July 2008

Downloaded from <http://pubs.acs.org> on February 8, 2009



### More About This Article

Additional resources and features associated with this article are available within the HTML version:

- Supporting Information
- Links to the 1 articles that cite this article, as of the time of this article download
- Access to high resolution figures
- Links to articles and content related to this article
- Copyright permission to reproduce figures and/or text from this article

[View the Full Text HTML](#)

## Zn Modification of the Reactivity of Pd(111) Toward Methanol and Formaldehyde

Eseoghene Jerero and John M. Vohs\*

Department of Chemical and Biomolecular Engineering, University of Pennsylvania, Philadelphia, Pennsylvania 19104-6363

Received January 7, 2008; E-mail: vohs@seas.upenn.edu

**Abstract:** The adsorption and reaction of methanol and formaldehyde on two-dimensional PdZn alloys on a Pd(111) surface were studied as a function of the Zn content in the alloy in order to understand the role of Zn in Pd/ZnO catalysts for the steam reforming of methanol (SRM). Temperature programmed desorption (TPD) and high resolution electron energy loss spectroscopy (HREELS) data show that Zn atoms incorporated into the Pd(111) surface dramatically decrease the dehydrogenation activity and alter the preferred bonding sites for adsorbed CO, CH<sub>3</sub>O, and CH<sub>2</sub>O intermediates. The experimental results obtained in this study are consistent with previous theoretical studies of this system and provide new insight into how Zn alters the reactivity of Pd.

### Introduction

Recently there has been much interest in the use of fuel cells as highly efficient energy conversion devices. Since many types of fuel cells use hydrogen as the fuel, this interest has motivated research into the development of renewable methods to produce H<sub>2</sub>. One method for H<sub>2</sub> production that has been proposed is the steam reforming of methanol or ethanol which can be produced using biorenewable resources. Highly selective catalysts that are active for the steam reforming reactions (e.g., CH<sub>3</sub>OH + H<sub>2</sub>O → CO<sub>2</sub> + 3H<sub>2</sub>) at low temperatures are needed, however, for this approach to be viable. The current state of the art catalyst for steam reforming of methanol (SRM) is Cu supported on ZnO<sup>1–3</sup> which exhibits both high activity and selectivity to H<sub>2</sub> and CO<sub>2</sub>. Unfortunately there are issues with the stability of Cu/ZnO catalysts since they are pyrophoric once reduced and Cu is prone to sintering at relatively low temperatures.<sup>4,5</sup> This latter property makes them not particularly amenable for use in distributed power applications.

Pd/ZnO has emerged as a possible alternative catalyst for SRM that does not suffer from some of the drawbacks of the copper-based system.<sup>6,7</sup> Pd/ZnO has also been shown to be active for ethanol steam reforming.<sup>8</sup> Iwasa et al. were the first to report that Pd/ZnO catalysts are active for SRM, exhibiting unusually high selectivity (>95%) for the production of CO<sub>2</sub>

and H<sub>2</sub> at 493 K.<sup>6</sup> The high selectivity to CO<sub>2</sub> relative to CO is important since the latter is a poison for the electrode catalysts used in polymer exchange membrane fuel cells (PEMFCs), one of the leading fuel cell technologies. The high selectivity to CO<sub>2</sub> is quite interesting in light of the fact that SRM over bulk Pd produces exclusively CO and H<sub>2</sub>.<sup>3,6,7,9–12</sup>

The dramatic change in the selectivity of Pd for SRM upon supporting it on ZnO has been attributed at least in part to the formation of a PdZn alloy under reaction conditions.<sup>1,6,13–15</sup> However, a mechanistic understanding of why the PdZn alloy exhibits such different reactivity compared to pure Pd is still lacking. Based on comparisons between Cu and Ag and group VIII metals, Takezawa and Iwasa<sup>6</sup> have suggested that one possible explanation is that Zn addition to Pd alters the bonding configuration of adsorbed aldehyde intermediates. On Cu and Ag, CH<sub>2</sub>O adsorbs in an η<sup>1</sup>-configuration in which the carbonyl is perpendicular to the surface and only the oxygen interacts with the metal<sup>16–18</sup> (see Figure 1a). The adsorption energies of η<sup>1</sup>-CH<sub>2</sub>O on Cu and Ag surfaces are relatively low, and CH<sub>2</sub>O desorbs below 140 K during temperature programmed desorption (TPD).<sup>19</sup> In contrast, on group VIII metals such as Pd, CH<sub>2</sub>O adsorbs in an η<sup>2</sup>-configuration in which the carbonyl group is parallel to the surface and both the C and O atoms

- (1) Wang, Y. H.; Zhang, J. C.; Xu, H. Y.; Bai, X. F. *Chin. J. Catal.* **2007**, *28*, 234.
- (2) Fukahori, S.; Kitaoka, T.; Tomoda, A.; Suzuki, R.; Wariishi, H. *Appl. Catal., A* **2006**, *300*, 155.
- (3) Kamata, H.; Takahashi, K.; Ibashi, W.; Komaki, H. *Stud. Surf. Sci. Catal.* **2003**, *145*, 479.
- (4) Zhang, C.; Yuan, Z.; Liu, N.; Wang, S.; Wang, S. *Fuel Cells*. **2006**, *6*, 466.
- (5) Jung, K. D.; Joe, O. S.; Han, S. H.; Uhm, S. J.; Chung, I. J. *Catal. Lett.* **1995**, *35*, 303.
- (6) Takezawa, N.; Iwasa, N. *Catal. Today*. **1997**, *36*, 45.
- (7) Iwasa, N.; Nomura, W.; Mayanagi, T.; Fujita, S.; Arai, M.; Takezawa, N. *J. Chem. Eng. Jpn.* **2004**, *37*, 286.
- (8) Casanovas, A.; Llorca, J.; Homs, N.; Fierro, J. L. G.; de la Piscina, P. R. *J. Mol. Catal. A: Chem.* **2006**, *250*, 44.

- (9) Iwasa, N.; Masuda, S.; Ogawa, N.; Takezawa, N. *Appl. Catal., A* **1995**, *125*, 145.
- (10) Chin, Y. H.; Dagle, R.; Hu, J. L.; Dohnalkova, A. C.; Wang, Y. *Catal. Today*. **2002**, *77*, 79.
- (11) Chin, Y. H.; Wang, Y.; Dagle, R. A.; Li, X. H. S. *Fuel Process. Technol.* **2003**, *83*, 193.
- (12) Cubeiro, M. L.; Fierro, J. L. G. *J. Catal.* **1998**, *179*, 150.
- (13) Wang, Y. H.; Zhang, J. C.; Xu, H. Y. *Chin. J. Catal.* **2006**, *27*, 217.
- (14) Bera, P.; Vohs, J. M. *J. Chem. Phys.* **2006**, *125*, 164713.
- (15) Iwasa, N.; Mayanagi, T.; Masuda, S.; Takezawa, N. *React. Kinet Catal. L.* **2000**, *69*, 355.
- (16) Fleck, L. E.; Ying, Z. C.; Feehery, M.; Dai, H. L. *Surf. Sci.* **1993**, *296*, 400.
- (17) Sexton, B. A.; Hughes, A. E.; Avery, N. R. *Surf. Sci.* **1985**, *155*, 366.
- (18) Wachs, I. E.; Madix, R. J. *Surf. Sci.* **1979**, *84*, 375.
- (19) Mavrikakis, M.; Barteau, M. A. *J. Mol. Catal. A: Chem.* **1998**, *131*, 135.

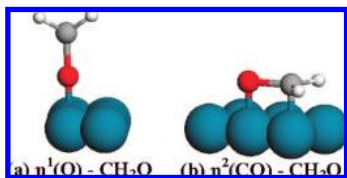


**Figure 1.** Adsorption configurations for  $\text{CH}_2\text{O}$  on Pd: (a)  $\eta^1(\text{O})\text{-CH}_2\text{O}$  and (b)  $\eta^2(\text{CO})\text{-CH}_2\text{O}$ .

bond to the metal<sup>20,21</sup> (Figure 1b). These species rapidly undergo dehydrogenation, and on Pd(111),  $\text{CH}_2\text{O}$  decomposes to CO and  $\text{H}_2$  at temperatures below 200 K.<sup>20</sup> Based on these observations and the similarity in the activity of Cu/ZnO and Pd/ZnO catalysts, Takezawa and Iwasa have proposed that on the PdZn alloy  $\text{CH}_2\text{O}$  also bonds in an  $\eta^1$ -configuration. This stabilizes it from dehydrogenation and allows for further reaction with hydroxyl groups to produce formate species which ultimately decompose to  $\text{CO}_2$  and  $\text{H}_2$ .<sup>6</sup>

While altering the preferred bonding configuration of adsorbed aldehyde intermediates is a plausible mechanism for how Zn affects reactivity, this hypothesis is not consistent with recent density functional theory (DFT) calculations for the interaction of  $\text{CH}_2\text{O}$  with PdZn(111) surfaces that indicate that  $\eta^2\text{-CH}_2\text{O}$  is still the most stable species.<sup>22,23</sup> These theoretical results also show that the barrier for breaking a C–H bond in an adsorbed methoxide group on PdZn(111) is 80 kJ/mol higher than that on Pd(111). This suggests that rather than altering the bonding configurations of reaction intermediates, the role of Zn may be to alter the barriers for C–H bond cleavage, thereby stabilizing methoxide and formaldehyde intermediates on the surface to higher temperatures.

The goal of the present study was to provide molecular-level insight into the adsorption sites, adsorption geometry, and reaction of both methanol and formaldehyde on PdZn alloy surfaces and to elucidate how Zn incorporation into the Pd surface alters the bonding configuration and stability of reaction intermediates. The adsorption and reaction of methanol and formaldehyde on model catalysts consisting of two-dimensional PdZn alloys with varying Zn content on the surface of a Pd(111) single crystal were characterized, using a combination of TPD and high resolution electron energy loss spectroscopy (HREELS). The experimental results obtained in this study along with comparisons to recently published DFT calculations for PdZn(111) surfaces<sup>23,24</sup> provide considerable new insight into how Zn addition alters the interaction of  $\text{C}_1$  oxygenates with the Pd(111) surface.

## Experimental Methods

The experiments were carried out in an ultrahigh vacuum (UHV) chamber with a background pressure of  $2 \times 10^{-10}$  Torr. The chamber was equipped with an ion sputter gun for sample cleaning, a quadrupole mass spectrometer (UTI) for TPD studies, a quartz crystal film thickness monitor (Maxtek Inc.) for monitoring the flux from the zinc metal deposition source, a retarding field electron energy analyzer (OCI Vacuum Microengineering) that was used for Low Energy Electron Diffraction (LEED), and a High Resolu-

tion Electron Energy Loss (HREEL) spectrometer (LK Technologies). A heating rate of 3 K/s was used in the TPD experiments, and the HREELS experiments were performed with an incident electron beam energy of 4 eV directed  $60^\circ$  from the surface normal and a resolution of  $\sim 5 \text{ cm}^{-1}$ .

The Pd(111) crystal used in this study was  $10 \text{ mm} \times 5 \text{ mm} \times 1 \text{ mm}$  in size. The temperature was measured using a chromel-alumel thermocouple that was spot-welded onto the back of the sample. Cleaning of the Pd(111) sample was accomplished by repeated cycles of 2 kV argon ion bombardment, followed by annealing at 1150 K for 25 s. The absence of impurities on the sample surface was confirmed using a combination of HREELS, LEED, and TPD. For TPD and HREELS experiments, the sample was cooled to  $\sim 100 \text{ K}$  using liquid nitrogen.

Zn was deposited onto the Pd(111) surface using an evaporative Zn source consisting of a short length of 0.5 mm diameter, high-purity Zn wire wrapped around a 0.2 mm diameter tungsten filament. The tungsten filament was attached to an electrical feedthrough on the UHV system and heated resistively. The Zn flux from the source was monitored using the quartz crystal film thickness monitor. Since Zn forms ordered surface layers on Pd(111), Zn coverages determined using the film thickness monitor were also confirmed via LEED analysis as reported previously.<sup>25</sup> We report Zn coverages as effective monolayers where one monolayer was assumed to be of  $1.53 \times 10^{15} \text{ atoms/cm}^2$  which is the density of Pd atoms on the Pd(111) surface.

The adsorbates,  $\text{CH}_3\text{OH}$  and  $\text{CH}_2\text{O}$ , used in this study were introduced into the chamber through a variable leak valve that was attached to a 5 mm stainless steel tube that the sample was positioned in front of during dosing. The  $\text{CH}_3\text{OH}$  (Alfa Aesar, 99.9%) was purified using multiple freeze–pump–thaw cycles prior to use, and the  $\text{CH}_2\text{O}$  was produced by heating a tube containing solid paraformaldehyde (Aldrich 95%) to induce depolymerization.

## Results

**Structure of Zn/Pd(111).** In previous studies the structure of Zn-covered Pd(111) surfaces has been studied in detail using low energy electron diffraction (LEED), X-ray photoelectron Spectroscopy (XPS), and CO TPD.<sup>24–28</sup> Based on angle-resolved XPS measurements, Bayer et al. determined that vapor-deposited Zn atoms on Pd(111) become incorporated into the Pd lattice upon heating between 300 and 650 K forming an ordered surface PdZn alloy.<sup>27</sup> Annealing to higher temperatures results in diffusion of Zn into the bulk of the Pd sample.<sup>26,27</sup>

The spatial arrangement of the Zn atoms in the PdZn alloys on the Pd(111) surface for several Zn coverages have been determined by LEED.<sup>25,27</sup> Annealing Pd(111) samples covered with 0.5 to 1.0 ML of Zn to 550 K produces a surface which exhibits a  $p(2 \times 1)$  LEED pattern, corresponding to a structure in which the surface consists of alternating rows of Pd and Zn atoms as shown schematically in Figure 2. Annealing a Zn/Pd(111) sample with a 0.25 ML Zn coverage to 550 K results in a surface which exhibits a similar LEED pattern which has been interpreted to be due to a  $p(2 \times 2)$  arrangement of the Zn atoms as shown in Figure 2.<sup>25</sup> Note that while the LEED pattern for the 0.25 ML Zn coverage could also be attributed to a surface containing islands of  $p(2 \times 1)$  domains, this interpretation is

(20) Davis, J. L.; Barteau, M. A. *J. Am. Chem. Soc.* **1989**, *111*, 1782.

(21) Davis, J. L.; Barteau, M. A. *Surf. Sci.* **1990**, *235*, 235.

(22) Chen, Z. X.; Lim, K. H.; Neyman, K. M.; Rosch, N. *J. Phys. Chem. B* **2005**, *109*, 4568.

(23) Lim, K. H.; Chen, Z. X.; Neyman, K. M.; Rosch, N. *J. Phys. Chem. B* **2006**, *110*, 14890.

(24) Chen, Z. X.; Neyman, K. M.; Lim, K. H.; Rosch, N. *Langmuir* **2004**, *20*, 8068.

(25) Jeroro, E.; Lebarbler, V.; Datye, A.; Wang, Y.; Vohs, J. M. *Surf. Sci.* **2007**, *601*, 5546.

(26) Gabasch, H.; Knop-Gericke, A.; Schlögl, R.; Penner, S.; Jenewein, B.; Hayek, K.; Klotzer, B. *J. Phys. Chem. B* **2006**, *110*, 11391.

(27) Bayer, A.; Flechtner, K.; Denecke, R.; Steinruck, H. P.; Neyman, K. M.; Rosch, N. *Surf. Sci.* **2006**, *600*, 78.

(28) Chen, Z. X.; Neyman, K. M.; Gordienko, A. B.; Rosch, N. *Phys. Rev. B* **2003**, *68*, 075417.

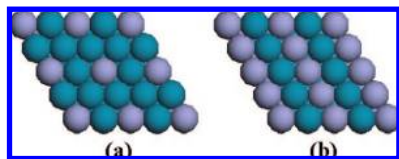


**Figure 2.** Models of (a) 0.25 ML  $p(2 \times 2)$ -Zn/Pd(111) and (b) 0.5 ML  $p(2 \times 1)$ -Zn/Pd(111).

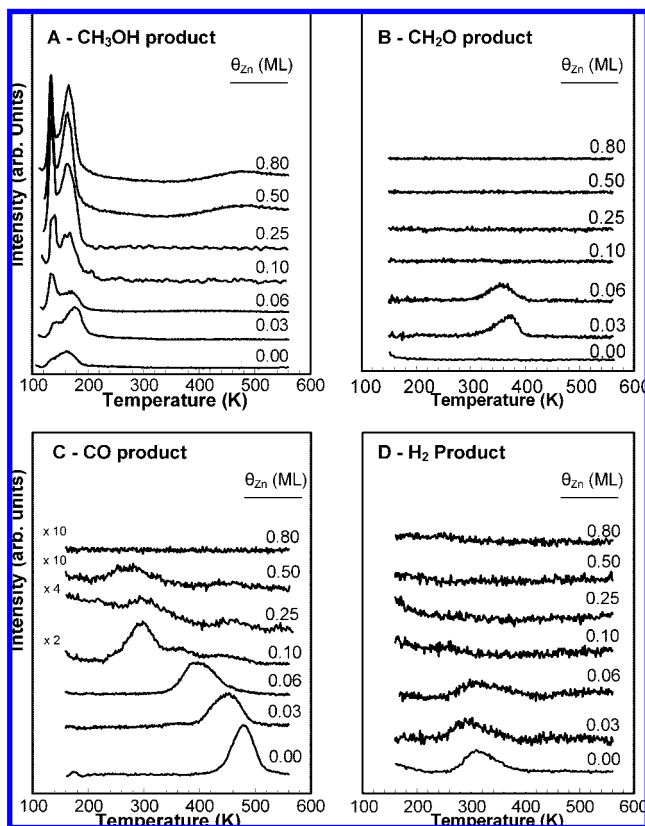


**Figure 3.** TPD spectra for (a) CH<sub>3</sub>OH, (b) CH<sub>2</sub>O, (c) CO, and (d) H<sub>2</sub> obtained from Zn/Pd(111) dosed with 0.5 L of CH<sub>3</sub>OH as a function of the Zn coverage.

not consistent with CO TPD results which show a continuous decrease in the CO desorption temperature with increasing Zn coverage.<sup>25</sup>

Based on these previous results, the Zn/Pd(111) samples used in the present study were annealed at 550 K in order to induce formation of the ordered PdZn alloy surface. LEED was used to confirm that the 0.5 and 0.25 ML Zn surfaces exhibited the  $p(2 \times 1)$  and  $p(2 \times 2)$  LEED patterns as previously reported.<sup>26,27</sup> LEED was also used to characterize surfaces with Zn coverages less than 0.2 ML. LEED patterns obtained from these surfaces exhibited the hexagonal pattern expected for the Pd(111) surface except the spots were slightly less intense. There was also more diffuse scattering giving rise to a higher background. This result suggests that a less ordered arrangement of surface Zn atoms is produced at low coverages.

**Temperature Programmed Desorption.** TPD data obtained from CH<sub>3</sub>OH-dosed Zn/Pd(111) samples as a function of Zn coverage are presented in Figure 3. Panels A, B, C, and D in this figure correspond to desorption spectra for CH<sub>3</sub>OH, CH<sub>2</sub>O, CO, and H<sub>2</sub>, respectively, which were the only products detected. As noted above, the sample was annealed at 550 K after each Zn deposition in order to induce formation of the surface PdZn

alloy. A CH<sub>3</sub>OH dose of 0.5 L was used in each TPD run. On the Zn-free Pd(111) surface, CH<sub>3</sub>OH undergoes dehydrogenation to CO and H<sub>2</sub> below 300 K,<sup>21,29,30</sup> and the TPD spectra contain desorption-limited peaks for CO and H<sub>2</sub> centered at 480 and 300 K, respectively. A small amount of unreacted CH<sub>3</sub>OH also desorbs in a broad peak centered at 160 K.

The substitution of only 0.03 ML of Zn into the Pd(111) surface caused several changes in the CH<sub>3</sub>OH TPD spectra, with the most dramatic being the appearance of a CH<sub>2</sub>O peak at 370 K. Since this peak was also observed from CH<sub>2</sub>O-dosed surfaces (see below), it must be desorption limited. Other changes evident in the TPD spectra upon the addition of 0.03 ML of Zn include a decrease in the activity for the dehydrogenation of methanol, a decrease in the CO desorption temperature from 480 to 450 K, and a broadening of the H<sub>2</sub> desorption peak toward lower temperatures. The CH<sub>3</sub>OH desorption signal can also now be resolved into two peaks centered at 140 and 170 K. On clean Pd(111), CH<sub>3</sub>OH desorption peaks are also observed near these temperatures, and based on XPS and SIMS data the peak at 140 K has been assigned to desorption of molecularly adsorbed CH<sub>3</sub>OH, and the peak at 170 K has been assigned to recombination of CH<sub>3</sub>O and H.<sup>30,31</sup>

Increasing the Zn coverage to 0.06 ML resulted in a further decrease in the CH<sub>3</sub>OH dehydrogenation activity as evidenced by an increase in the amount of CH<sub>3</sub>OH desorbing from the surface, as well as decreases in the amounts of CO and H<sub>2</sub> produced. The CH<sub>3</sub>OH desorption signal is still composed of two peaks centered at 140 and 170 K, although the relative intensities of the peaks have changed with the lower-temperature peak now being more intense. The CH<sub>3</sub>OH peak at 140 K is also very narrow with a full width at half-maximum of only 20 K, which is consistent with a zero or half-order desorption process. The CO desorption peak has also further shifted to lower temperature and now appears to be composed of at least two overlapping peaks centered at ~400 K. For 0.06 ML of Zn the CH<sub>2</sub>O peak is still evident, although it has shifted to a slightly lower temperature of 360 K.

Dramatic changes in the CH<sub>3</sub>OH TPD results were again observed upon increasing the Zn coverage to 0.10 ML. The CH<sub>3</sub>OH dehydrogenation activity decreased significantly with the total amount of CO produced dropping by ~50%. The CO desorption signal was complex consisting of multiple overlapping peaks between 220 and 450 K, with the most intense peak centered at 300 K. Also at this Zn coverage, the CH<sub>2</sub>O desorption peak is no longer present. The data at higher Zn coverages in Figure 3 show a continued decrease in the CH<sub>3</sub>OH dehydrogenation activity with increasing Zn content. For the 0.25 and 0.5 ML Zn samples, only small amounts of CO were produced and desorbed primarily at 300 and 270 K, respectively. CH<sub>3</sub>OH does not undergo decomposition on the 0.8 ML Zn sample. The intensities of both of the CH<sub>3</sub>OH peaks at 140 and 170 K also increased with increasing Zn coverage, and for Zn coverages of 0.5 ML and higher, an additional broad CH<sub>3</sub>OH desorption feature centered near 450 K is present.

Since CH<sub>2</sub>O was one of the products during the reaction of CH<sub>3</sub>OH on Zn/Pd(111), TPD data for CH<sub>2</sub>O-dosed surfaces were also collected and are displayed in Figure 4. Panels A and B in this figure correspond to the CH<sub>2</sub>O and CO desorption signals, respectively. H<sub>2</sub> was also produced but is not shown in

(29) Gates, J. A.; Kesmodel, L. L. *J. Catal.* **1983**, *83*, 437.

(30) Davis, J. L.; Barteau, M. A. *Surf. Sci.* **1987**, *187*, 387.

(31) Chen, J. J.; Jiang, Z. C.; Zhou, Y.; Chakraborty, B. R.; Winograd, N. *Surf. Sci.* **1995**, *328*, 248.



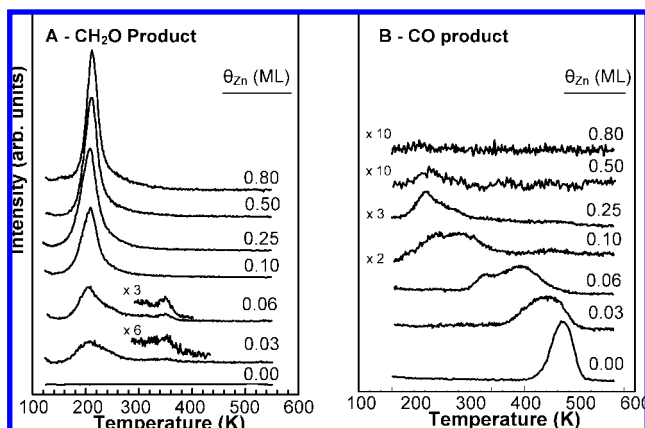


**Figure 4.** TPD spectra for (a) CH<sub>2</sub>O and (b) CO obtained from Zn/Pd(111) dosed with 0.5 L of CH<sub>2</sub>O as a function of the Zn coverage.

the figure. A CH<sub>2</sub>O exposure of 0.5 L was used in each TPD run. Similar to CH<sub>3</sub>OH, CH<sub>2</sub>O decomposes on clean Pd(111) to CO and H<sub>2</sub><sup>20</sup> as shown in the bottom curves in Figure 4 where the only carbon-containing product is CO which desorbs at 470 K. The trends in the CH<sub>2</sub>O TPD results with Zn coverage are similar to those observed for CH<sub>3</sub>OH. In both cases increasing the Zn coverage caused decreases in the dehydrogenation activity and the CO desorption temperature. For Zn coverages between 0.06 and 0.25 ML, CO desorbs in a series of overlapping peaks between 200 and 450 K, and for 0.5 ML of Zn, the primary CO desorption peak is centered at 220 K. CO was not produced on the surface with 0.8 ML of Zn.

As was also the case for CH<sub>3</sub>OH, 0.03 ML of Zn was sufficient to cause a measurable decrease in the activity for CH<sub>2</sub>O dehydrogenation. For this Zn coverage, two CH<sub>2</sub>O peaks are observed at 210 and 360 K, with the lower-temperature peak being much more intense. Both of these peaks grew in intensity when the Zn coverage was increased to 0.06 ML. At higher Zn coverages only the low-temperature CH<sub>2</sub>O peak at 210 K was observed. The intensity of this peak continually increased with Zn coverage for coverages up to 0.8 ML.

**High Resolution Electron Energy Loss Spectroscopy.** HREELS was used to characterize adsorbed species on the CH<sub>3</sub>OH- and CH<sub>2</sub>O-dosed Zn/Pd(111) surfaces. Since the HREEL spectra from the CH<sub>2</sub>O-dosed surfaces are helpful in assigning the peaks in the spectra for the CH<sub>3</sub>OH-dosed surfaces, they will be presented first. HREEL spectra obtained from Zn/Pd(111) dosed with 0.5 L of CH<sub>2</sub>O as a function of Zn coverage are shown in Figure 5, and peak assignments are listed in Table 1. In this set of experiments, CH<sub>2</sub>O was dosed with the sample at 100 K, followed by briefly heating to 150 and then 200 K. The sample was then allowed to cool back to 100 K, and the spectrum was collected. The bottom spectrum in both panels corresponds to the Zn-free Pd(111) surface and contains prominent peaks centered at 940, 1120, 1205, 1460, and 1860 cm<sup>-1</sup>. These spectra are similar to that reported previously for CH<sub>2</sub>O on Pd(111) at temperatures below 240 K by Davis and Barteau.<sup>20</sup> The peak at 1860 cm<sup>-1</sup> is characteristic of the  $\nu(\text{CO})$  mode of CO adsorbed in 3-fold hollow sites on the Pd(111) surface<sup>32,33</sup> and demonstrates that a portion of the adsorbed CH<sub>2</sub>O undergoes dehydrogenation to CO and H<sub>2</sub> at temperatures

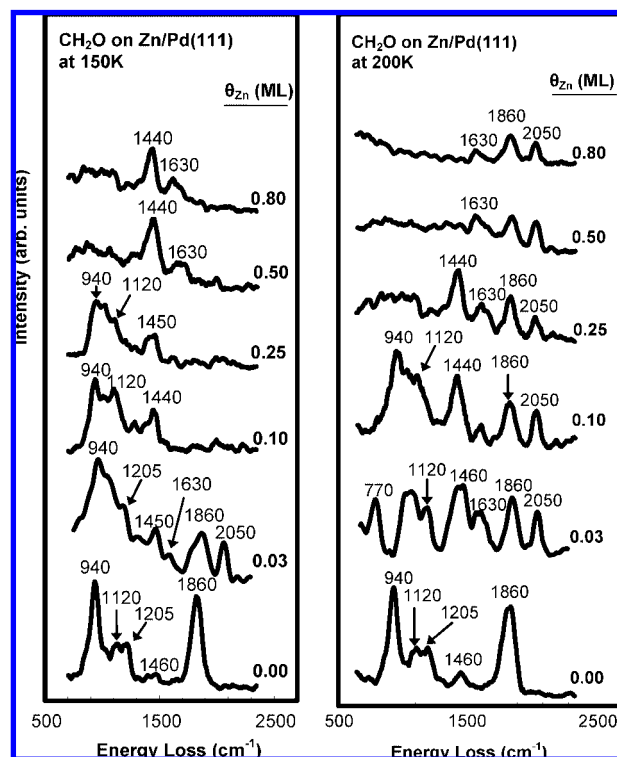


**Figure 5.** HREEL spectra of Zn/Pd(111) dosed with 0.5 L of CH<sub>2</sub>O at 100 K after heating to 150 and 200 K.

**Table 1.** HREELS Peak Assignments for CH<sub>2</sub>O-Dosed Zn/Pd(111)

mode	surface species	frequency, cm <sup>-1</sup>					
		Pd(111)	0.3 ML Zn/Pd	0.1 ML Zn/Pd	0.25 ML Zn/Pd	0.5 ML Zn/Pd	0.8 ML Zn/Pd
$\nu(\text{CO})$	CO atop		2050	2050	2050 <sup>b</sup>	2050 <sup>b</sup>	2050 <sup>b</sup>
$\nu(\text{CO})$	CO 3-fold	1860	1860	1860	1860 <sup>b</sup>	1860 <sup>b</sup>	1860 <sup>b</sup>
$\nu(\text{CO})$	$\eta^1\text{-CH}_2\text{O}$		1630	1630	1630 <sup>b</sup>	1630	1630
$\nu(\text{CO})$	$\eta^2\text{-CH}_2\text{O}$	1460	1450	1440	1440	1440 <sup>a</sup>	1440 <sup>a</sup>
$\rho(\text{CH}_2)$	CH <sub>2</sub> O	1205	1205 <sup>a</sup>	1205	1205 <sup>a</sup>		
$\nu_s(\text{OCO})$	(CH <sub>2</sub> O) <sub>n</sub>	1120	1120	1120	1120 <sup>a</sup>		
$\nu_s(\text{OCO})$	(CH <sub>2</sub> O) <sub>n</sub>	940		940	940 <sup>a</sup>		
$\pi(\text{CO})$	$\eta^2\text{-CH}_2\text{O}$		770 <sup>b</sup>				

<sup>a</sup> Observed only at 150 K. <sup>b</sup> Observed only at 200 K.

below 200 K. Based on comparisons to the IR spectra of gaseous CH<sub>2</sub>O and solid paraformaldehyde (CH<sub>2</sub>O)<sub>n</sub>, Davis and Barteau assigned the peaks at 940 and 1120 cm<sup>-1</sup> to the symmetric and asymmetric O–C–O stretching modes of adsorbed paraformaldehyde and the peak at 1205 cm<sup>-1</sup> to the  $\rho(\text{CH}_2)$  mode of adsorbed molecular CH<sub>2</sub>O. The peak at 1460 cm<sup>-1</sup> is at an energy consistent with that reported for CH<sub>2</sub>O adsorbed in an  $\eta^2$  configuration on group VIII metal surfaces.<sup>6</sup>

The incorporation 0.03 ML of Zn into the Pd(111) surface caused several changes in the HREEL spectrum of the CH<sub>2</sub>O-dosed surface at 150 K, with more significant changes observed upon heating to 200 K. Spectra obtained at both temperatures show an increase in the intensity of the  $\eta^2\text{-}\nu(\text{CO})$  peak at 1460 cm<sup>-1</sup> and the appearance of new peaks at 1630 and 2050 cm<sup>-1</sup>. The latter peak can be assigned to the  $\nu(\text{CO})$  mode of CO adsorbed atop Pd atoms.<sup>32</sup> This peak is slightly lower in intensity than the peak at 1860 cm<sup>-1</sup> corresponding to CO adsorbed in 3-fold hollow sites. As will be discussed below, a shift in the preferred bonding configuration of adsorbed CO from 3-fold to atop sites is consistent with that reported in our previous study of the interaction of CO with Zn/Pd(111) surfaces.<sup>25</sup> The

(32) Kuhn, W. K.; Szanyi, J.; Goodman, D. W. *Surf. Sci.* **1992**, *274*, L611.  
 (33) Szanyi, J.; Kuhn, W. K.; Goodman, D. W. *J. Vac. Sci. Technol., A* **1993**, *11*, 1969.

new peak at  $1630\text{ cm}^{-1}$  is at an energy close to that reported by Davis and Barteau for the  $\nu(\text{CO})$  mode of  $\text{CH}_2\text{O}$  adsorbed in an  $\eta^1$  configuration.<sup>21</sup> Similar peak positions for the  $\nu(\text{CO})$  mode of  $\eta^1$ - $\text{CH}_2\text{O}$  have also been reported for other transition metal surfaces.<sup>34</sup>

Heating the 0.03 ML Zn/Pd(111) sample to 200 K caused an increase in the intensity of both  $\nu(\text{CO})$  peaks of adsorbed  $\text{CH}_2\text{O}$ , with the  $\eta^1$  peak at  $1630\text{ cm}^{-1}$  being roughly half the size of the  $\eta^2$  peak at  $1450\text{ cm}^{-1}$ . Since the C–O bond in the  $\eta^2$  configuration will be nearly parallel to the surface, while that in the  $\eta^1$  configuration is perpendicular to the surface, dipole selection rules dictate that the cross section for exciting the  $\nu(\text{CO})$  mode in the  $\eta^1$  species will be significantly larger than that for the  $\eta^2$  species. Thus, based on the peak areas, the  $\eta^2$  configuration is still the primary bonding geometry for  $\text{CH}_2\text{O}$  on the 0.03 ML Zn/Pd(111) surface at 200 K. Nonetheless it appears that one effect of the addition of Zn to the surface is to stabilize bonding of  $\text{CH}_2\text{O}$  in the  $\eta^1$  configuration relative to that on the Zn-free surface. Additional peak assignments for the  $\text{CH}_2\text{O}$ -dosed 0.03 ML Zn/Pd(111) surface at 150 and 200 K are listed in Table 1.

HREEL Spectra for the  $\text{CH}_2\text{O}$ -dosed 0.1 and 0.25 ML Zn/Pd(111) samples at 150 K show the disappearance of the peaks at  $1630$ ,  $1860$ , and  $2050\text{ cm}^{-1}$ . At these Zn coverages and temperature, the spectrum only contains peaks that can be assigned to paraformaldehyde and  $\eta^2$ - $\text{CH}_2\text{O}$  (see Table 1). Heating the sample to 200 K results in the reappearance of the peak at  $1630\text{ cm}^{-1}$ , suggesting some interconversion between the  $\eta^2$  and  $\eta^1$ - $\text{CH}_2\text{O}$  species. The peaks at  $1860$  and  $2050\text{ cm}^{-1}$ , corresponding to CO adsorbed in the 3-fold hollow and atop Pd sites, also reappear. These results show that dehydrogenation of adsorbed  $\text{CH}_2\text{O}$  occurs at a higher temperature on the 0.1 ML Zn/Pd(111) surface relative to the clean Pd(111) surface, suggesting that the Zn causes an increase in the activation energy for this reaction.

More significant changes were observed upon increasing the Zn coverage to 0.5 and 0.8 ML. At 150 K, the peak at  $1630\text{ cm}^{-1}$  corresponding to the  $\nu(\text{CO})$  mode of  $\eta^1$ - $\text{CH}_2\text{O}$  reappears, signifying the coexistence of  $\eta^2$ - and  $\eta^1$ - $\text{CH}_2\text{O}$  species. Heating to 200 K results in the disappearance of the peak at  $1440\text{ cm}^{-1}$  corresponding to the  $\nu(\text{CO})$  mode of  $\eta^2$ - $\text{CH}_2\text{O}$ . The peak at  $1630\text{ cm}^{-1}$  is still readily apparent at these Zn coverages, however, as is the  $\nu(\text{CO})$  peak for CO adsorbed in 3-fold and atop sites. The overall intensity of the adsorbate peaks also decreased significantly at 200 K, indicating a decrease in the total amount of adsorbed species on these surfaces.

HREEL spectra obtained from Zn/Pd(111) dosed with 0.5 L of  $\text{CH}_3\text{OH}$  as a function of Zn coverage and temperature are shown in Figure 6, and peak assignments are listed in Table 2. In this set of experiments prior to collecting each spectrum, the sample was again dosed at 100 K, briefly heated to 150 and then 200 K to desorb molecularly adsorbed  $\text{CH}_3\text{OH}$ , and then allowed to cool to 100 K at which point the HREEL spectrum was collected. The bottom spectrum in both panels corresponds to the Zn-free Pd(111) surface. At 150 K, the most prominent features in the spectrum are peaks at  $1005$  and  $1450\text{ cm}^{-1}$ , which can be attributed to the  $\nu(\text{CO})$  and  $\delta(\text{CH}_3)$  modes of adsorbed methoxide groups ( $\text{CH}_3\text{O}$ ).<sup>21</sup> The  $\delta(\text{CH}_3)$  peak position overlaps with that expected for the  $\nu(\text{CO})$  of  $\eta^2$ - $\text{CH}_2\text{O}$ , so the presence of some  $\text{CH}_2\text{O}$  on the surface can not be completely ruled out.

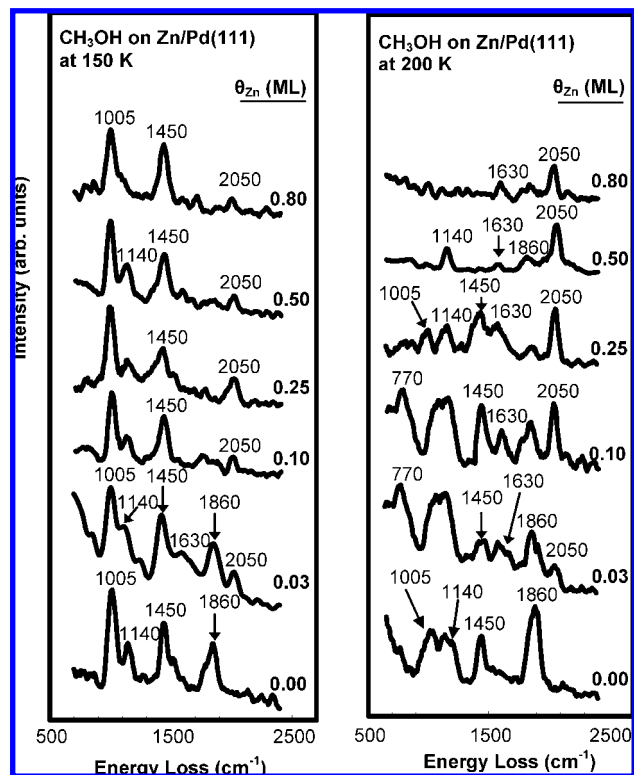


**Figure 6.** HREEL spectra of Zn/Pd(111) dosed with 0.5 L of  $\text{CH}_3\text{OH}$  at 100 K after heating to 150 and 200 K.

**Table 2.** HREELS Peak Assignments for  $\text{CH}_3\text{OH}$ -Dosed Zn/Pd(111)

mode	surface species	frequency, $\text{cm}^{-1}$					
		Pd(111)	0.03 ML Zn/Pd	0.1 ML Zn/Pd	0.25 ML Zn/Pd	0.5 ML Zn/Pd	0.8 ML Zn/Pd
$\nu(\text{CO})$	CO atop		2050	2050	2050	2050	2050
$\nu(\text{CO})$	CO 3-fold	1860	1860	1860	1860 <sup>b</sup>	1860 <sup>b</sup>	1860 <sup>b</sup>
$\nu(\text{CO})$	$\eta^1$ - $\text{CH}_2\text{O}$		1630	1630 <sup>b</sup>	1630 <sup>b</sup>	1630	1630
$\nu(\text{CO})$	$\eta^2$ - $\text{CH}_2\text{O}$	1450	1450	1450	1450	1450 <sup>a</sup>	1450 <sup>a</sup>
$\eta(\text{CH}_3)$	$\text{CH}_3\text{O}$	1140	1140	1140	1140	1140	1140 <sup>a</sup>
$\nu(\text{CO})$	$\text{CH}_3\text{O}$	1005	1005	1005	1005	1005 <sup>a</sup>	1005 <sup>a</sup>
$\pi(\text{CO})$	$\eta^2$ - $\text{CH}_2\text{O}$		770 <sup>b</sup>	770 <sup>b</sup>			

<sup>a</sup> Observed only at 150 K. <sup>b</sup> Observed only at 200 K.

Additional peaks are also evident at  $1140$  and  $1860\text{ cm}^{-1}$  which can be assigned to the  $\rho(\text{CH}_3)$  mode of methoxide groups and the  $\nu(\text{CO})$  mode of CO on 3-fold hollow sites, respectively. The presence of the CO peak demonstrates that a fraction of the adsorbed  $\text{CH}_3\text{OH}$  undergoes complete dehydrogenation at temperatures below 150 K.

Heating the Zn-free Pd(111) surface to 200 K results in the decrease in the intensity of the methoxide peaks at  $1005$  and  $1450\text{ cm}^{-1}$  which is consistent with the TPD results which show that  $\text{CH}_3\text{OH}$  desorbs between 150 and 200 K. An increase in the intensity of the  $\nu(\text{CO})$  peak of 3-fold CO at  $1860\text{ cm}^{-1}$  is also evident, indicating that additional methoxide groups underwent dehydrogenation.

Several changes are evident upon the addition of small amounts of Zn to the Pd(111) surface. For 0.03 ML of Zn at 150 K, the spectrum is similar to that for clean Pd(111) except that C–O stretches for both 3-fold ( $1860\text{ cm}^{-1}$ ) and atop ( $2050\text{ cm}^{-1}$ ) CO are observed. A peak at  $1630\text{ cm}^{-1}$  is also resolvable and can be attributed to the  $\nu(\text{CO})$  mode of  $\eta^1$ - $\text{CH}_2\text{O}$ . Again it is possible that  $\eta^2$ - $\text{CH}_2\text{O}$  species are present, since its  $\nu(\text{CO})$

(34) Anton, A. B.; Parmeter, J. E.; Weinberg, W. H. *J. Am. Chem. Soc.* **1986**, *108*, 1823.

peak overlaps with the  $\delta(\text{CH}_3)$  peak of methoxide. Heating this surface to 200 K resulted in decreases in the intensities of the peaks at 1005 and 1450  $\text{cm}^{-1}$  and the appearance of a peak at 770  $\text{cm}^{-1}$  which can be attributed to the  $\pi(\text{CO})$  mode of  $\eta^2\text{-CH}_2\text{O}$ .<sup>21</sup> While there appears to still be some methoxide groups on the surface, the peaks at 770, 1450, and 1630  $\text{cm}^{-1}$  suggest that, in addition to CO, the primary adsorbed species are  $\eta^1$ - and  $\eta^2\text{-CH}_2\text{O}$ .

Increasing the Zn coverage to 0.1 ML and then 0.25 ML produced changes in the peaks associated with adsorbed  $\text{CH}_2\text{O}$  species. At 150 K the peak at 1630  $\text{cm}^{-1}$ , assigned to the  $\nu(\text{CO})$  mode of  $\eta^1\text{-CH}_2\text{O}$ , disappears for both Zn coverages. Thus at 150 K for these Zn coverages, only the  $\eta^2\text{-CH}_2\text{O}$  species are formed. The peak characteristic of  $\eta^1\text{-CH}_2\text{O}$  (1630  $\text{cm}^{-1}$ ) reappears, however, upon heating to 200 K where peaks indicative of both  $\eta^1$ - and  $\eta^2\text{-CH}_2\text{O}$  are observed in each spectrum. At this temperature, changes were also observed in the region associated with adsorbed CO where the intensity of the peak at 1860  $\text{cm}^{-1}$  due to 3-fold CO decreased with increasing Zn coverage, while that for atop CO at 2050  $\text{cm}^{-1}$  remained nearly constant. These results are consistent with both a decrease in the dehydrogenation activity of the surface and a preference for CO to bond in atop sites versus 3-fold sites with increasing Zn coverage. Further increases in the Zn coverage to 0.5 and then 0.8 ML caused little change in the spectra at 150 K, and these spectra were dominated by features due to adsorbed methoxide groups. However at 200 K, significant decreases in the intensity of the adsorbate vibrational peaks are observed, which is again indicative of the decrease in dehydrogenation activity with increasing Zn coverage.

The TPD results for both  $\text{CH}_3\text{OH}$  and  $\text{CH}_2\text{O}$ -dosed Zn/Pd(111) with low Zn coverages (0.03 and 0.06 ML) contain a  $\text{CH}_2\text{O}$  desorption peak near 360 K. To provide insight into the surface species that gives rise to this TPD peak, an HREEL spectrum of the  $\text{CH}_3\text{OH}$ -dosed 0.03 ML Zn/Pd(111) surface that had been briefly heated to 300 K was also collected. This spectrum along with that of the surface heated to 200 K is shown in Figure 7. While the spectra are similar, there is a difference in the relative intensities of the  $\nu(\text{CO})$  peaks for the  $\eta^1$ - and  $\eta^2\text{-CH}_2\text{O}$  species with the latter (1440  $\text{cm}^{-1}$ ) increasing relative to the former (1630  $\text{cm}^{-1}$ ) as the surface was heated to 300 K. As noted above, the cross section for exciting the  $\nu(\text{CO})$  mode in the  $\eta^2$ -species is significantly larger than that in the  $\eta^1$ -species. Thus, the spectrum at 300 K suggests that  $\eta^2$  is the primary bonding configuration for  $\text{CH}_2\text{O}$  on the 0.03 ML Zn/Pd(111) surface at 300 K. These results seem to suggest that the high-temperature  $\text{CH}_2\text{O}$  feature in the TPD spectra corresponds to the desorption of the  $\eta^2\text{-CH}_2\text{O}$  species.

## Discussion

The TPD results for both  $\text{CH}_2\text{O}$  and  $\text{CH}_3\text{OH}$  show that the addition of Zn to the Pd(111) surface influences the reactivity and the preferred bonding sites for adsorbed species. The most obvious influence on reactivity is an overall decrease in the extent of dehydrogenation of adsorbed  $\text{CH}_3\text{O}$  and  $\text{CH}_2\text{O}$  species with increasing Zn coverage. This is evident by the data in Figure 8, where the amount of CO produced (in monolayers) during TPD for a constant 0.5 L dose of either  $\text{CH}_2\text{O}$  or  $\text{CH}_3\text{OH}$  is plotted as a function of Zn coverage. On clean Pd(111) both  $\text{CH}_2\text{O}$  and  $\text{CH}_3\text{OH}$  undergo nearly complete dehydrogenation to produce adsorbed CO and hydrogen atoms at temperatures below 250 K. For Zn coverages up to 0.06 ML, the decrease in the amount of CO produced is relatively small but drops

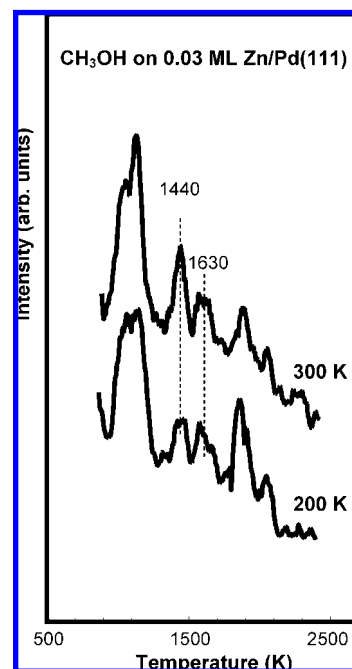


**Figure 7.** HREEL spectra of 0.03 ML Zn/Pd(111) dosed with 0.5 L of  $\text{CH}_3\text{OH}$  at 100 K after heating to 200 and 300 K.

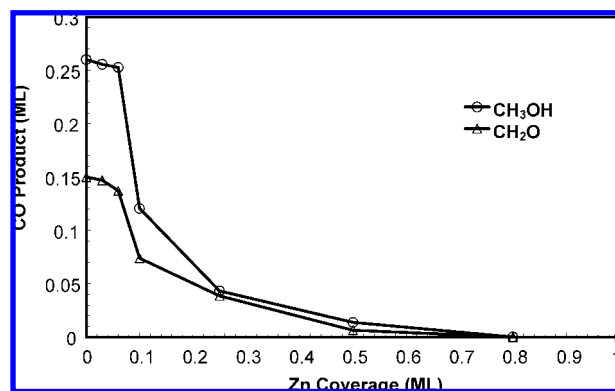


**Figure 8.** Amount of CO produced in monolayers for Zn/Pd(111) dosed with 0.5 L of  $\text{CH}_3\text{OH}$  as a function of the Zn coverage.

precipitously at 0.1 ML and asymptotically approaches zero for Zn coverages above 0.5 ML.

Previous DFT calculations of the interaction of  $\text{CH}_3\text{O}$  groups with Pd and PdZn surfaces provide insight that is useful in explaining the reactivity trends observed in the present study.<sup>24,35</sup> Unlike other group VIII metals where atop sites are the lowest energy binding sites for methoxide groups, DFT calculations indicate that on Pd(111) methoxide groups prefer 3-fold hollow sites.<sup>24,35</sup> Chen et al. report that the average adsorption energy on these sites is 158  $\text{kJ mol}^{-1}$  (average of the energies for the hcp and fcc 3-fold hollow sites).<sup>24</sup> They also found that 3-fold hollows were the most stable adsorption sites on PdZn(111). The calculated adsorption energies for  $\text{CH}_3\text{O}$  on PdZn<sub>2</sub> and Pd<sub>2</sub>Zn 3-fold sites on this surface are 221 and 194  $\text{kJ mol}^{-1}$ , respectively. This shows that the O in the methoxide group prefers to bind to as many Zn atoms as possible. Chen et al. have also reported the reaction and activation energies for breaking a C–H bond in the methoxide group to produce

(35) Kua, J.; Goddard, W. A. *J. Am. Chem. Soc.* **1999**, *121*, 10928.



adsorbed  $\text{CH}_2\text{O}$  and H. On Pd(111) the reaction energy is exothermic by  $45 \text{ kJ mol}^{-1}$ , while on PdZn(111) it is endothermic by  $61 \text{ kJ mol}^{-1}$ . There are also large differences in the activation energies for this reaction with the calculated values being only  $33 \text{ kJ mol}^{-1}$  on Pd(111) but  $113 \text{ kJ mol}^{-1}$  on PdZn(111).

These theoretical results predict that on the surfaces used in the present investigation the most stable binding sites for methoxide groups will be 3-fold hollows that include one or two Zn atoms, and that methoxide groups adsorbed on these sites will be significantly less prone to undergo dehydrogenation than those adsorbed on 3-fold hollows containing only Pd atoms. These results also predict that the dehydrogenation activity should decrease rapidly with Zn coverage since each surface Zn atom creates multiple Zn-containing 3-fold sites. As shown in Figures 3 and 8, this is indeed the case. For the 0.06 ML Zn surface, where 90% of the 3-fold hollow sites are still composed of three Pd atoms, only a small decrease in the extent of dehydrogenation of adsorbed methoxide species is observed. In contrast, on the 0.25 ML Zn surface, which has a  $p(2 \times 2)$  structure, 25% of the 3-fold sites are composed of three Pd atoms, while the remaining 75% are composed of two Pd atoms and one Zn atom. Assuming that the 0.5 L dose produced a constant coverage of methoxide species on the two surfaces (this assumption is supported by the TPD data) the data in Figure 8 show that the fraction of methoxide groups that underwent dehydrogenation on the 0.25 ML Zn surface decreased by  $\sim 80\%$  relative to Zn-free Pd(111).

DFT calculations by Chen et al. on the interaction of  $\text{CH}_2\text{O}$  with the PdZn surface<sup>23,24</sup> also help explain the reduced dehydrogenation activity toward  $\text{CH}_2\text{O}$  with Zn addition. These calculations show that, on the Pd(111) and PdZn(111) surfaces,  $\text{CH}_2\text{O}$  prefers to bond in the  $\eta^2$  configuration with adsorption energies of  $-43$  and  $-23 \text{ kJ mol}^{-1}$ , respectively. On PdZn(111), they found the most stable  $\eta^2$  configuration was with the C and O atoms bonded to adjacent Pd and Zn sites. In the Chen work, reaction energies for H abstraction from  $\text{CH}_2\text{O}$  were reported to be exothermic by  $56 \text{ kJ mol}^{-1}$  on Pd(111), but by only  $4 \text{ kJ mol}^{-1}$  on PdZn(111).<sup>23</sup> Large differences were also observed in the activation energies for this reaction with calculated values of  $38 \text{ kJ mol}^{-1}$  for Pd(111) and  $64 \text{ kJ mol}^{-1}$  on PdZn(111).<sup>23</sup> The formation of the alloy almost doubles the activation energy, showing that H abstraction on the PdZn alloy is unlikely. These theoretical results are consistent with the experimental results obtained in the present study which also show that surfaces that contain equal numbers of Pd and Zn atoms are nearly inactive for the dehydrogenation of adsorbed  $\text{CH}_2\text{O}$ .

The theoretical studies by Chen et al. also indicate that  $\eta^1$  is not a stable bonding configuration for  $\text{CH}_2\text{O}$  on PdZn(111).<sup>23,24</sup> This is not completely consistent with the HREELS data obtained in the present study where  $\eta^1\text{-CH}_2\text{O}$  species were observed for all Zn coverages including the 0.5 ML Zn/Pd(111) sample. On  $\text{CH}_2\text{O}$ -dosed surfaces the coverage of  $\eta^1\text{-CH}_2\text{O}$  species was always relatively small, however, and the  $\eta^1 \nu(\text{CO})$  peak was largely insensitive to the Zn coverage, unlike that for  $\eta^2\text{-CH}_2\text{O}$ . These trends were also observed for the  $\text{CH}_3\text{OH}$ -dosed surfaces. This suggests that the  $\eta^1\text{-CH}_2\text{O}$  species is not an important reaction intermediate and may be formed at a small number of defect sites on the surface. These results also argue against the hypothesis of Takezawa and Iwasa<sup>6</sup> that one function of Zn in the PdZn-alloy SRM catalyst is to stabilize the bonding of adsorbed  $\text{CH}_2\text{O}$  in the  $\eta^1$ -configuration, since both the

experimental and theoretical results indicate that the  $\eta^2$  bonding configuration dominates on the alloy surface.

An interesting feature of the TPD results for both  $\text{CH}_3\text{OH}$  and  $\text{CH}_2\text{O}$  reactants is the presence of the  $\text{CH}_2\text{O}$  peak near 360 K for Zn/Pd(111) surfaces with low Zn coverages (0.03 and 0.06 ML). As discussed above, the HREELS results, while not providing a definitive assignment of the surface species that gives rise to this feature, strongly suggest that it results from the desorption of  $\eta^2\text{-CH}_2\text{O}$ . This is a surprising result since at higher Zn coverages nearly all of the  $\eta^2\text{-CH}_2\text{O}$  desorbs at 210 K. Based on comparison to the Chen et al. theoretical studies,<sup>24</sup> the 210 K desorption peak can be assigned to  $\text{CH}_2\text{O}$  adsorbed on Pd–Zn sites with the oxygen bonded to Zn and the carbon bonded to Pd. It is tempting to assign the  $\text{CH}_2\text{O}$  that desorbs at 360 K to similar isolated Pd–Zn sites, but it is not clear why the adsorption energy would be so much higher on these sites unless the number of nearest neighbor zincs is important. It is also possible that Zn atoms adjacent to Pd–Pd sites decrease the dehydrogenation activity on these sites, thereby stabilizing molecularly adsorbed  $\text{CH}_2\text{O}$  to higher temperatures. The fact that in the Chen et al. study the adsorption energy for  $\eta^2\text{-CH}_2\text{O}$  on Pd(111) is nearly twice that on PdZn(111) adds some support to this hypothesis. For Pd(111) the higher adsorption energy for  $\text{CH}_2\text{O}$  does not manifest itself in the TPD results, since adsorbed formaldehyde undergoes dehydrogenation at temperatures below 200 K.

The  $\text{CH}_3\text{OH}$  and  $\text{CH}_2\text{O}$  TPD data also show significant variations in the CO desorption temperature with Zn coverage. Note that, on Pd(111), CO produced by dehydrogenation of adsorbed  $\text{CH}_3\text{O}$  and  $\text{CH}_2\text{O}$  desorbs in a single peak centered at 480 K. The CO desorption temperature decreases with increasing amounts of Zn incorporated into the surface, and for Zn coverages greater than 0.25 ML, CO desorbs below 300 K. The HREELS results also show that the stability of CO bound in atop sites relative to 3-fold hollow sites increases with increasing Zn coverage. For the  $\text{CH}_3\text{OH}$ -dosed surfaces only 3-fold CO was detected on Pd(111), while atop species dominated for Zn coverages greater than 0.1 ML.

The trends observed for the interaction of CO produced by dehydrogenation of  $\text{CH}_3\text{OH}$  and  $\text{CH}_2\text{O}$  with the Zn/Pd(111) surfaces are nearly identical to those reported in our previous HREELS and TPD study of the adsorption of CO on these surfaces.<sup>25</sup> In that study it was shown that carbon monoxide interacts only weakly with exposed Zn atoms on the alloy surface and at temperatures above 100 K and does not adsorb on sites that contain Zn. In addition to this ensemble effect, Zn was also shown to have a strong electronic effect that destabilizes the bonding of CO on nearby Pd-only sites. This is evident in the TPD results of the present study by comparing the CO desorption spectra from the  $\text{CH}_2\text{O}$ -dosed Pd(111) and 0.03 ML Zn/Pd(111) surfaces (see Figure 4). Note that the HREELS results show that although CO adsorbs primarily on 3-fold hollow sites on both of these surfaces, there is a noticeable decrease in the CO desorption temperature with Zn addition. The perturbation of the electronic properties of Pd by Zn which give rise to these effects is also clearly evident in XPS studies of PdZn alloys.<sup>14,26,36</sup>

In our previous study it was shown that the heat of adsorption of CO was destabilized by  $16 \text{ kJ/mol}$  on 3-fold Pd sites that have Zn next-nearest neighbors compared to 3-fold sites on the clean Pd(111) surface. It was also found that Zn incorporation

(36) Rodriguez, A. *J. Phys. Chem.* **1994**, *98*, 5758.



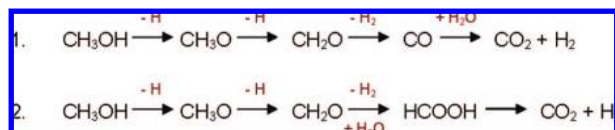


Figure 9. Proposed pathways for steam reforming of methanol on PdZn.

into Pd(111) shifts the preferred bonding configuration of CO from 3-fold hollow and bridge sites to atop sites. Finally it should be noted that these conclusions for the interaction of CO with Zn/Pd(111) surfaces are consistent with predictions based on DFT calculations<sup>22</sup> and with trends reported for high surface area catalysts.<sup>25</sup>

Before discussing the implications of the results obtained in this study for the mechanism of SRM on PdZn alloy catalysts, it is useful to first consider the reaction pathways for the conversion of methanol and water to CO<sub>2</sub> and H<sub>2</sub>. The most likely pathways are those shown in Figure 9. Pathway 1 proceeds via complete dehydrogenation of adsorbed methoxide groups followed by the water gas shift (WGS) reaction to convert the CO to CO<sub>2</sub>. Pathway 2 proceeds via dehydrogenation of methoxide to produce formaldehyde (or formyl) that then reacts with adsorbed water or hydroxyl groups to produce formate, which ultimately decompose to CO<sub>2</sub> and H<sub>2</sub>. As has been pointed out previously by Takezawa and Iwasa,<sup>6</sup> pathway 1 is unlikely since the observed selectivity to CO<sub>2</sub> during SRM over Pd/ZnO is well beyond the equilibrium selectivity obtainable by the WGS reaction.

Assuming that SRM proceeds according to pathway 2, the experimental results obtained in the present study have multiple implications for understanding the role of Zn in PdZn catalysts. First they strongly suggest that the SRM reaction would not proceed on surfaces containing a high concentration of Zn. The barrier for C–H bond scission on these surfaces is prohibitively high and the preferred pathway for methoxide groups is recombinative desorption as methanol. Indeed as shown in Figure 3 during methanol TPD on Zn/Pd(111) surfaces with Zn coverages >0.1 ML, this is the preferred pathway and occurs well below room temperature. We have recently performed TPD experiments in which methanol and water were coadsorbed on a 0.25 ML Zn/Pd(111) surface which provide additional support for this conclusion. The presence of water (or hydroxyl groups) had little effect on the reactivity of adsorbed methoxides which still desorbed as methanol at 170 K.

Second the results of this study suggest that a stabilized form of  $\eta^2$ -CH<sub>2</sub>O may be an important intermediate in SRM on PdZn. On Zn/Pd(111) surfaces with low Zn coverages (<0.1 ML)  $\eta^2$ -CH<sub>2</sub>O remains stable from dehydrogenation and desorbs intact at 360 K. This is in contrast to clean Pd(111) where  $\eta^2$ -CH<sub>2</sub>O undergoes complete dehydrogenation below room temperature. It is likely that under typical SRM conditions, the Zn-stabilized form of  $\eta^2$ -CH<sub>2</sub>O would remain on the surface at sufficiently high temperatures to react with hydroxyl groups to form formate. Based on this scenario, the role of Zn is not to alter the bonding configuration of adsorbed reactants and intermediates as proposed by Iwasa,<sup>6</sup> but rather to increase the barrier for C–H bond scission in adsorbed formaldehyde thereby shutting down the dehydrogenation pathway that produces CO. At low Zn coverages the barrier for C–H bond scission in methoxides either remains unchanged or increases slightly but not enough to preclude formation of formaldehyde. The effect for  $\eta^2$ -CH<sub>2</sub>O is much more dramatic and the C–H bond scission barrier for

this moiety is increased sufficiently to make  $\eta^2$ -CH<sub>2</sub>O a stable surface intermediate.

It is also interesting to use the insights obtained in this study to speculate on the structure of the active sites in high surface area SRM catalysts. Based solely on the results reported here one might conclude that PdZn alloys with relatively low Zn concentrations would be the most active and selective. This is not completely consistent with what is observed experimentally, however, since catalysts with average Pd/Zn ratios of 1:1 can exhibit high selectivity to CO<sub>2</sub> and H<sub>2</sub>.<sup>10,37</sup> On the other hand, a recent study by Karim et al.<sup>38</sup> reports that for Pd/ZnO catalysts the selectivity to CO<sub>2</sub> during SRM does not correlate with the extent of alloy formation and that catalysts with both high and low extents of alloying of Zn with Pd exhibit high selectivity to CO<sub>2</sub>. This result in conjunction with those obtained here suggests that the surface concentration of Zn in supported PdZn alloy particles may deviate significantly from that in the bulk. Since the results of the present study indicate that the relevant chemistry may be taking place on Pd surfaces with relatively low Zn concentrations, one also needs to consider whether the active sites consist of defects or step edges that are decorated with Zn atoms. While more study is needed to definitively answer this question, our results for the interaction of CO with Zn/Pd(111) argue against it. Note that for the 0.03 ML Zn surface the desorption temperature for CO in 3-fold hollow sites decreases by 30 K (see Figure 3).<sup>25</sup> For this low coverage if Zn was merely decorating defect sites you would expect the majority of the 3-fold sites to be unaltered and the CO TPD spectrum would contain a CO peak at 480 K which is characteristic of clean Pd(111) and a much smaller feature at the lower temperature resulting from CO desorption from the Zn-altered defect sites. There is also some data in the literature for high surface area catalysts which suggest that the primary role of Zn in PdZn SRM catalysts is not to simply alter chemistry near defect sites. These studies<sup>38,39</sup> have shown that the selectivity of PdZn SRM catalysts increases with particle size and that low selectivity is obtained from catalysts with average particle sizes < 2 nm. Thus, the particles that would be expected to have the highest concentration of defects and other under-coordinated sites are the least selective.

Finally it should be noted that the observation that very low coverages of Zn have a profound effect on the surface reactivity of Pd is a surprising result and provides motivation for additional theoretical studies of this effect. To date, theoretical DFT studies of this system have focused almost exclusively on surfaces of the stoichiometric PdZn alloy, which as discussed above may not be very active for SRM. DFT studies of systems with much lower concentrations of Zn, while being more challenging computationally, may also provide more insight into the role of Zn in the PdZn alloy. Since alloying is commonly used in supported metals catalysis, the results of this investigation also provide more general motivation to study the reactivity of the extremes of alloy compositions, since this may be where the relevant chemistry occurs.

## Conclusions

The incorporation of Zn into the Pd(111) surface was found to significantly affect the adsorption and reaction of CH<sub>3</sub>OH and CH<sub>2</sub>O. One of the most obvious effects of Zn addition is

(37) Xia, G.; Holladay, J. D.; Dagle, R. A.; Jones, E. O.; Wang, Y. *Chem. Eng. Technol.* **2005**, *28*, 515.

(38) Karim, A.; Conant, T.; Datye, A. *J. Catal.* **2006**, *243*, 420.

(39) Dagle, R. A.; Chin, Y. H.; Wang, Y. *Top. Catal.* **2007**, *46*, 358.

to decrease the propensity of adsorbed  $\text{CH}_2\text{O}$  and  $\text{CH}_3\text{O}$  species to undergo dehydrogenation to produce CO and  $\text{H}_2$ . This decrease in the dehydrogenation activity is quite dramatic and is observed for Zn coverages as low as 0.03 ML. The extent of dehydrogenation of adsorbed  $\text{CH}_2\text{O}$  and  $\text{CH}_3\text{O}$  species during TPD dropped by roughly 50% on surfaces with only 0.1 ML of Zn and was nearly absent on surfaces with 0.5 ML of Zn. The activation energy for the dehydrogenation reactions was also found to increase with increasing Zn coverage.

The experimental results obtained in this study in conjunction with the theoretical results of Chen et al.<sup>23,24</sup> indicate that the oxygen atom in methoxide species prefers to interact with surface Zn and the most stable bonding site for methoxide groups on Zn/Pd(111) surfaces are 3-fold hollows containing one or two Zn atoms. The activation energy for dehydrogenation of methoxide groups adsorbed on these sites is higher than that on Pd-only sites, and during TPD their primary reaction pathway is recombination with adsorbed hydrogen to produce methanol. The primary bonding configuration for adsorbed  $\text{CH}_2\text{O}$  was found to be the  $\eta^2$  configuration in which both the C and O atoms interact with the surface. On surfaces containing Zn, the most stable binding sites for  $\text{CH}_2\text{O}$  appear to be Pd–Zn dimers on which the carbon end of the molecule bonds to the Pd and the oxygen end bonds to Zn. As was also the case for methoxide groups, the activation energy for dehydrogenation of adsorbed  $\text{CH}_2\text{O}$  is higher on the Pd–Zn sites relative to Pd–Pd sites.

Consistent with our previous study, the incorporation of Zn into Pd(111) was found to influence the interaction of CO with the surface through both electronic and ensemble effects. Through-surface electronic effects are evident by the destabilization of CO adsorbed on Pd 3-fold hollow sites with Zn nearest neighbors relative to those on Zn-free Pd(111), while ensemble effects cause the preferred CO binding site to change from 3-fold hollows to atop Pd atoms. Finally the results of this study are not consistent with the hypothesis of Takezawa and Iwasa<sup>6</sup> that one of the primary functions of Zn in PdZn alloy SRM catalysts is to stabilize the  $\eta^1$  bonding configuration of adsorbed  $\text{CH}_2\text{O}$  intermediates relative to the  $\eta^2$  configuration. While  $\eta^1$ - $\text{CH}_2\text{O}$  species were observed on the Zn/Pd(111) surfaces,  $\eta^2$ - $\text{CH}_2\text{O}$  was the dominant species on all of the surfaces studied, suggesting that it is the intermediate involved in the SRM on Pd/ZnO catalysts. Hence, the significant increase of the barrier for C–H scission from  $\eta^2$ - $\text{CH}_2\text{O}$  is most likely responsible for the decreased dehydrogenation activity observed on the PdZn surface.

**Acknowledgment.** Funding for this study was provided by the U.S. Department of Energy (Grant No. DE-FG02-05ER15712 and DE-FG02-04ER15605).

JA8001265